Proposed Modifications to Ice Accretion/Icing Scaling Theory

Alan J. Bilanin*
Continuum Dynamics, Inc., Princeton, New Jersey 08543

The difficulty of conducting full-scale icing tests has long been appreciated. Testing in an icing wind tunnel has been undertaken for decades. While aircraft size and speed have increased, tunnel facilities have not, thus making subscale geometric tests a necessity. Scaling laws governing these tests are almost exclusively based on analysis performed over 30 years ago and have not been rigorously validated. The following work reviews past scaling analyses and suggests revision to these analyses based on recent experimental observation. It is also suggested, based on the analysis contained herein, that current ice accretion predictive technologies, such as LEWICE, when utilized in the glaze ice accretion regime, may need upgrading to more accurately estimate the rate of ice buildup on aerodynamic surfaces.

Nomenclature

A_C	= accumulation factor
b	= relative heat factor
C	= chord or characteristic dimension
C_p	= specific heat
d	= cylinder diameter or drop diameter
E	= internal energy
h_c	= convective heat transfer coefficient
h_{fs}	= latent heat of fusion
k	= thermal conductivity
LWC	= liquid water content
ℓ	= mean spacing between drops
M	= mass
R	= drop radius
R_s	= radius of impacted drop
s	= arc length
T	= temperature
T_a	= air temperature
T_f	= freezing temperature
T_s	= surface temperature
t	= time
t_s	= thickness of impacted drop
U_∞	= freestream speed
α	= incidence angle
β	= local collection efficiency
γ	= contact angle
δ	= layer thickness
η	= freezing fraction
θ	= air driving potential
μ	= absolute viscosity
ν	= kinematic viscosity
ρ	= density
σ	= surface tension
τ	= shear stress
ϕ	= water driving potential

Subscripts

a	= air
w	= water
i	= ice

Presented as Paper 88-0203 at the AIAA 26th Aerospace Sciences Meeting, Reno, NV, Jan. 11–14, 1988; received April 8, 1988; revision received July 8, 1988.

*Senior Associate. Senior Member AIAA.

I. Introduction

NASA Lewis Research Center and the Federal Aviation Adminstration (FAA) are currently supporting efforts to develop analytic tools to estimate the rate of ice accretion on aerodynamic surfaces. Concurrently, these efforts are causing a re-examination of the rules under which icing tests are conducted in wind tunnels. Because of the inherent difficulties of documenting icing conditions in the atmosphere in which an aircraft will be flown and the costs associated with flight tests, the use of icing wind tunnels and subscale models is almost a necessity. Yet the basic physics of ice accretion is not readily understood, whereas the problem of ice accretion on aerodynamic surfaces has been known since nearly the earliest days of aviation. To illustrate this lack of detailed understanding, take, for instance, the nature of the ice accretions. Those that occur at atmospheric temperatures significantly below freezing at low speeds and liquid water contents that allow impacting droplets to freeze immediately upon impact with a surface are referred to as rime ice accretion. Conditions where both liquid and ice exist on the surface of the ice are referred to as glaze ice. These definitions of ice accretion types have been in use for some time now, yet there appears to be no quantitative definiton of these ice regimes. For example, what is the functional relationship between ambient temperature and velocity for droplet impact at a stagnation point that separates the rime ice accretion region from the glaze ice regime? To our knowledge, this question has not been answered.

One of several troublesome observations is associated with the actual impact of the supercooled droplets with the surface of the airfoil. Current analyses, and all previous analyses for that matter, assume that the impacting drop sticks to the surface and utilizes the collection efficiency schematically illustrated in Fig. 1. Recently, there has been an interest in the impact of rain with aerodynamic surfaces,[1] and although rain drops are significantly larger than supercooled icing droplets, a large fraction of the droplet mass that impacts the surface is

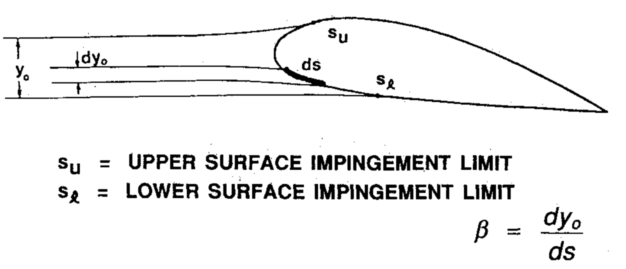

Fig. 1 Definition of local collection efficiency.

splashed back into the airstream.[2] The ratio of the surface energy to the kinetic energy of the drop prior to impact is

$$\frac{\sigma_{w/a}4\pi R^2}{\frac{1}{2}\rho_w \frac{4}{3}\pi R^3 U_\infty^2} = \frac{6\sigma_{w/a}}{\rho_w R U_\infty^2} \tag{1}$$

Assume an incoming droplet of diameter $2R = 30\ \mu\text{m}$ at 32°F and a droplet impact speed of 400 ft/s (the surface tension between water and air is approximately 0.5×10^{-2} lb/ft, this ratio is of the order of $\sigma(10^{-3})$. The kinetic energy is three orders of magnitude larger than the surface energy. If we now assume that all the kinetic energy goes into the surface energy of a droplet stuck to the surface, as shown in Fig. 2, and approximate the droplet by a right circular cylinder of radius R_s and thickness t_s, conservation of energy and mass yields

$$\frac{1}{2}\rho_w \frac{4}{3}\pi R^3 U_\infty^2 \simeq (10^3)4\pi R^2\sigma_{w/a} \simeq \pi R_s^2(\sigma_{w/a} + \sigma_{w/s})$$

$$\frac{4}{3}\pi R^3 = \pi t_s R_s^2 \tag{2}$$

By assuming that $\sigma_{w/a} \simeq \sigma_{w/s}$, a 30-$\mu$m drop will become a droplet on the impacted surface of diameter $2R_s = 1300\ \mu\text{m}$ with a thickness of $t_s \sim 10^{-2}\ \mu\text{m}$ or about 100 water molecules.

Admittedly, all the kinetic energy of impact does not go into increasing the surface area of the impacting droplet, but it seems hardly likely that these drops impact and do not splash back. The fact that to date there have been tens of investigators[3-5] who have methodically computed the collection efficiency about complex aerodynamic shapes by assuming that all of the impacted subcooled droplets impact the surface and either freeze immediately or are carried along the aerodynamic surface in a liquid film is somewhat surprising. Lastly, it is most curious that investigators of the ice accretion problem[6-8] to date have not considered the dynamics of the liquid film (although they most certainly acknowledge its presence), the physical mechanisms that determine its thickness, and the velocity of the water of which the film is made. Much discussion of this fact will be made in the following.

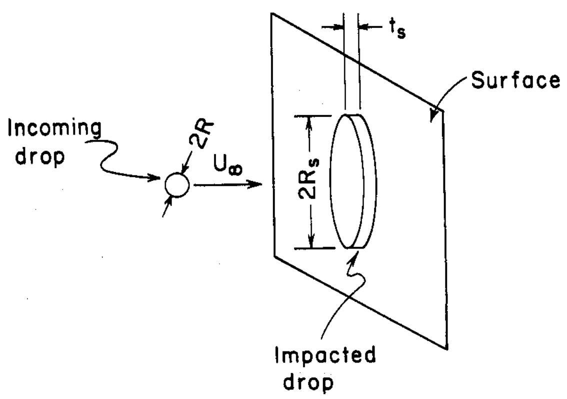

Fig. 2 Schematic of a water droplet impacting and adhering to a surface.

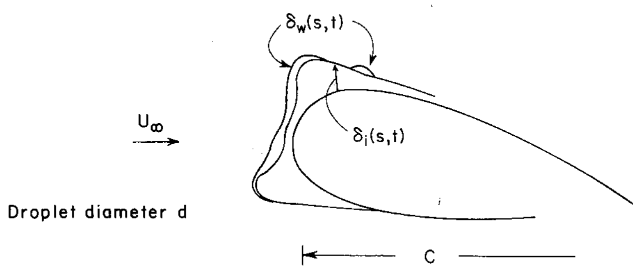

Fig. 3 Schematic of the ice accretion process.

II. Buckingham-π Analysis of Icing Scaling

A brute force approach to the problem of scaling ice accretion is attempted here to see if a set of similitude laws can be obtained. These tests are to be conducted at subscale and the results obtained are to be reliably extracted to full scale. Figure 3 schematically shows the ice accretion process on an airfoil of chord C. A test is to be conducted where the ice thickness $\delta_i(s, t)$ will be measured on the airfoil as a function of time. As has been assumed in the rain impact problem, evaporative processes are neglected.[9] During the encounter of an icing cloud, the air is nearly saturated, and the neglect of additional evaporation and condensation is likely a good approximation. In addition, as a simplification in the analysis, the heat capacity of the aerodynamic surface is assumed to be very small so that the thermal response of the structure can be neglected. Under these assumptions, the variables listed in Table 1 are assumed to influence the ice accretion process. Note that the water layer thickness δ_w is not a variable (although its presence is acknowledged) and does not enter the nondimensional groups that will be derived.

Straightforward application of the Buckingham-π theory yields the normalized thickness of the ice accreted on the airfoil as a function of 18 nondimensional groups. Hence,

$$\frac{\delta_i}{C} = f(\pi_1, \pi_2, \ldots, \ldots, \pi_{18}) \tag{3}$$

where

$$\pi_1 = \frac{tU_\infty}{C} \qquad \pi_2 = \frac{s}{C} \qquad \pi_3 = \frac{d}{C}$$

$$\pi_4 = \frac{d}{\ell} \qquad \pi_5 = \frac{\rho_a}{\rho_w} \qquad \pi_6 = \frac{\rho_i}{\rho_w}$$

$$\pi_7 = \frac{C_{pa}}{C_{pw}} \qquad \pi_8 = \frac{C_{pw}}{C_{pi}} \qquad \pi_9 = \frac{k_a}{k_w}$$

$$\pi_{10} = \frac{k_w}{k_i} \qquad \pi_{11} = \frac{v_a}{v_w} \qquad \pi_{12} = \gamma$$

$$\pi_{13} = \frac{C_{pa}v_a\rho_a}{k_a} \qquad \pi_{14} = \frac{T_f}{T_a} \qquad \pi_{15} = \frac{h_{fs}}{C_pT_a}$$

$$\pi_{16} = \frac{U_\infty^2}{C_pT_a} \qquad \pi_{17} = \frac{U_\infty C}{v_a} \qquad \pi_{18} = \frac{\rho_a U_\infty^2 C}{\sigma_{w/a}}$$

The implications of the π parameters are as follows. The first two parameters are independent variables and need no discussion. A reduction test airfoil dimension C requires that droplet size be reduced by the scale reduction factor, as well as the mean spacing between drops. Since water density is essentially a constant, parameters 3 and 4 require that the liquid water content be held constant between scaled tests. This is essentially the result obtained when scaling for testing subscale airfoils for heavy rain effects.[9] Parameters π_5–π_{13} are property ratios that can be readily matched between scaled tests, especially since water and air are the fluids used at all scales. The parameter π_{13} is the well-known Prandtl number, which measures the relative magnitudes of molecular and thermal transport. Parameter π_{14} requires that the ratio of the freezing temperature to the ambient temperature be held constant. This is equivalent to maintaining a constant temperature difference between scaled tests, but since the freezing temperature of water is a constant, this restriction requires all tests to be conducted at the same ambient temperature. If this is done, then the ratio of latent heat of fusion to acoustic speed squared, π_{15}, is automatically satisfied.

The next three parameters, π_{16}–π_{18}, require that the freestream velocity vary as

$$U_\infty = \text{const}, \qquad \theta_\infty \sim 1/C, \qquad U_\infty \sim 1/\sqrt{C}$$

Table 1 Variables

	Description	Units
Lengths		
$\delta_i(s, t)$	Ice thickness	L
d	Drop diameter	L
ℓ	Mean distance between drops	L
C	Chord	L
Densities		
ρ_a	Air	M/L^3
ρ_w	Water	M/L^3
ρ_i	Ice	M/L^3
Viscosity		
ν_a	Air	L^2/T
ν_w	Water	L^2/T
Thermal		
k_a	Thermal conductivity air	$ML/T^{3°}$
k_w	Thermal conductivity water	$ML/T^{3°}$
k_i	Thermal conductivity ice	$ML/T^{3°}$
C_{pa}	Specific heat air	$L^2/T^{2°}$
C_{pw}	Specific heat water	$L^2/T^{2°}$
C_{pi}	Specific heat ice	L^2/T^{20}
h_{fs}	Latent heat fusion	L^2/T^2
T_a	Air temperature	°
T_f	Freezing temperature	°
Surface tension		
$\sigma_{w/a}$	Water/air	M/T^2
γ	Droplet contact angle	M/T^2
Velocity		
U_∞	Air speed	L/T
s	Distance along airfoil	L
t	Time	T

Table 2 Prior scaling analysis

Ref.	Scaling analysis	Scaling parameters held constant A_C	η	b	ϕ	θ
13	Douglas Aircraft	X				
14	Lockheed Aircraft	X	X	X		
15	Boeing Aircraft	X				
16	British Aircraft	X	X	X		
17	ONERA	X	X	X	X	X
18	AEDC	X	X		X	X

respectively, in an attempt to keep the Mach, Reynolds, and Weber numbers constant between scaled tests. Obviously this is not possible, and not surprisingly the π method has failed to provide a scaling methodology that can be used to test subscale aerodynamic components. Curiously, by this approach, no methodology is identified that may be used during full-scale ground tests, such as those performed on engines,[10] which will allow a tradeoff of uncontrolled ambient conditions.

In summary, the preceding discussion implies that although there are many π parameters that are automatically satisfied at subscale, there exists a problem holding Mach, Reynolds, and Weber numbers constant between tests. Not surprising, however, is that the complex phenomenon of ice accretion is not a phenomenon that may be exactly scaled. This, however, does not preclude seeking approximate scaling methodologies, the subject of the discussion to follow.

III. Past Scaling Laws

Almost without exception, past analysis of ice accretion scaling can be cast in a form that states that the rate at which ice grows at a point on an aerodynamic surface is proportional to the liquid inflow to this point times the fraction of this liquid that freezes. (This is known as the freezing fraction η.) For convenience, this analysis has been explicitly written down in the vicinity of a stagnation point as shown in Fig. 4, and the generalization for other locations along the airfoil is straightforward. The accretion rate at a stagnation point is, therefore,

$$\frac{\mathrm{d}(\delta_i/C)}{\mathrm{d}(tU_\infty/C)} = \frac{LWC\beta\eta}{\rho_i} \tag{4}$$

where $LWC = \rho_w(\mathrm{d}/\ell)^3$ and β is the collection efficiency. The freezing fraction η is defined as the mass freezing/mass water incoming. Note that Eq. (4) is nondimensional; exact and scaled ice accretion exactly requires that

$$\frac{LWC\beta}{\rho_i}\frac{tU_\infty}{C}\eta = A_C\eta = \text{const}$$

or that accumulation parameter A_C and η each be held constant, which is what is normally attempted. The η, which is nondimensional, is not one of the basic π variables defined, yet if it were accurately estimated from an analytical model as a function of the variables discussed, scaling laws for ice accretion could be deduced. The freezing fraction has been computed by several investigators using a model proposed by Messinger in 1951.[11] If evaporation is neglected in this model,

$$\eta = \left(\phi + \frac{\theta}{b}\right)(C_{pw}/h_{fs}) \tag{5}$$

where

$$\phi = T_f - T_\infty - (U^2/2C_{pw})$$

$$\theta = T_s - T_\infty - (U^2/2C_{pa})$$

$$b = \text{relative heat factor } (LWC\beta U_\infty C_{pw}/h_c)$$

This is essentially the functional form of freezing fraction used in the SIMICE code.[12] Several authors have reviewed the basis of η, and it is not the purpose here to once again argue the control volume heat balance upon which it is based. It is important to note, however, that momentum transport from the air to the liquid film, which must exist, and the surface tension phenomenon are explicitly omitted in the derivation.

Table 2 shows the past application of the described scaling methodology. Note that all researchers agree that A_C must be held constant between scales, yet both Douglas and Boeing do not attempt to hold freezing fraction constant between tests. Note also that it is assumed in the derivation of the accumulation factor that all incident droplets are either frozen or transported in a water film on the surface. Splashing is implicitly assumed not to exist in the current scaling method-

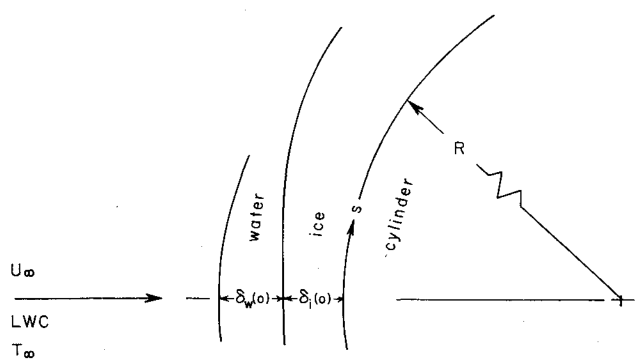

Fig. 4 Schematic of ice accretion at a stagnation point (not to scale).

Table 3 Selected test data

Test	LWC, g^3	η_m	η_T
1	1.2	0.35	0.15
2	0.8	0.35	0.15
3	1.2	0.6	0.5
4	0.8	0.6	0.5

ologies. Even more surprising is the fact that four other investigators attempt to hold some combinations of the additional parameters b, θ, and ϕ constant as well as η, even though there is no physical basis to do so. The fact that, to date, no one is claiming an acceptable scaling methodology suggests that acceptable agreement with scaled data has yet to be obtained. This is illustrated next.

IV. Brief Examination of Data

The following discussion will consider ice accretion at the stagnation point of a circular cylinder as shown in Fig. 4. This location is selected since it represents the location at which fluid flow conditions are most readily known and, therefore, in principle, is most easily modeled. The growth of ice thickness at the stagnation point $s = 0$ is exactly

$$\frac{\delta_i(o)}{2R} = A_C \eta \tag{6}$$

Therefore, conducting several experiments where A_C and η are individually held constant between experiments, or the product of $A_C\eta$ is held constant, should give geometrically scaled ice accretions. It is again emphasized that if A_C and η are accurately computed analytically and held constant between two tests, the prediction of ice accretion and scaling of

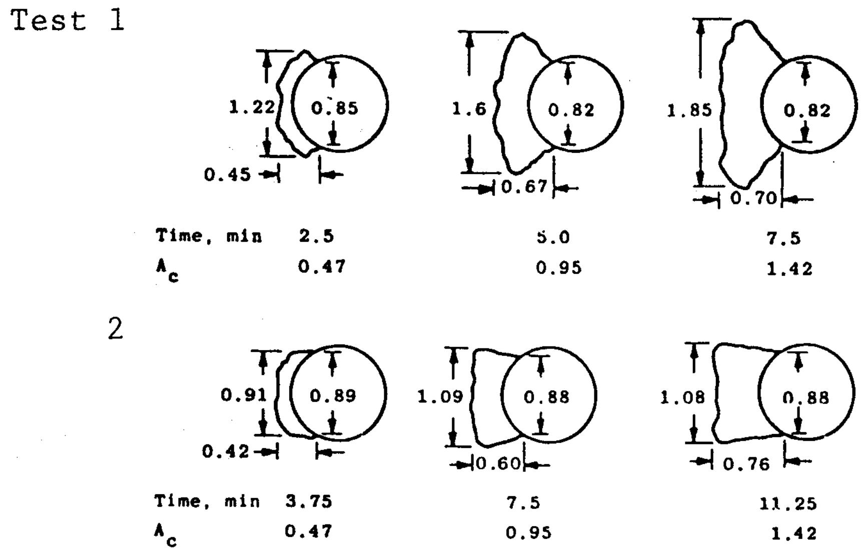

		LWC, g/m³	U_∞, fps	T_s, °F	P_s, psia	$\bar{d}m$, μm	K_0	n	b	ϕ, °F	θ, °F
1	1.0-in.-diam	1.2	200	23	14.2	20	2.29	0.15	0.78	8.2	10.9
2	1.0-in.-diam	0.8	200	24.8	14.2	20	2.29	0.15	0.52	6.4	8.2

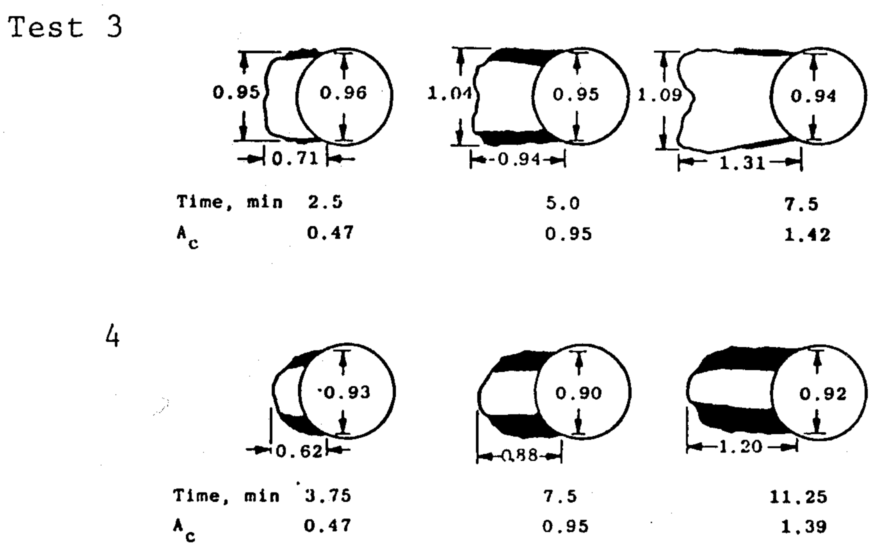

		LWC, g/m³	U_∞, fps	T_s, °F	P_s, psia	$\bar{d}m$, μm	K_0	n	b	ϕ, °F	ϕ, °F
3	1.0-in.-diam	1.2	200	5	14.2	20	2.29	0.50	0.83	26.2	35.5
4	1.0-in.-diam	0.8	200	11.5	14.2	20	2.29	0.50	0.54	19.7	27.2

Fig. 5 Ice accretion on a 1-in.-diam circular cylinder.[18]

icing tests is a proven technology. To see that this is not the case, we have taken data obtained by Ruff[18] shown in Fig. 5 and have plotted the thickness of the ice accretion at the stagnation point $\delta_i(o)/2R$ vs accumulation parameter A_C (see Fig. 6). These four tests are significant in that tunnel speed and the cylinder are common. Hence, the Reynolds number based on cylinder diameter is a constant between the experiments. As can be seen from Fig. 5, the slope of the data is the measured freezing fraction η_T, and the predicted theoretical freezing fractions using the SIMICE scaling code[12] are tabulated in the legend. The results are shown in Table 3.

Obviously something is very wrong here, since at lower freezing fractions the theoretical SIMICE freezing fraction differs from the measured value by a factor of 2.3. The problem is that the freezing fraction η in Eq. (5) is not being computed to sufficient accuracy using the Messinger formulation.

As the freezing fraction approaches zero, it is to be anticipated that liquid film dynamics dominate the transfer of shear stress to the surface from the airstream. Yet this transport mechanism is omitted from all accretion models reviewed. Also, not surprising then is the fact that theoretical ice accretions are in greatest error when $\eta \to 0$ and large amounts of liquid water are transported about the airfoil surface.

V. Film Dynamics at a Stagnation Point

An investigation of scaling laws for testing under heavy rain conditions[9] led to a simple integral theory for film thickness that involves the solution of two equations:

$$\delta_w U = \frac{2LWCU_\infty}{\rho_w} s \sin\alpha \tag{7}$$

$$\frac{d}{ds}(\delta_w U^2) = \frac{LWCU_\infty^2}{\rho_w}\sin\alpha\cos\alpha + \frac{\tau(\delta)}{\rho_w} - v_w\frac{U}{\delta_w} + U_o\frac{\partial U_o}{\partial s}s \tag{8}$$

As an example, Eqs. (7) and (8) may be written for the local stagnation point flow around a cylinder (Fig. 4) where U is the water velocity at the air/water interface, U_o the air velocity along the surface, s the distance along the surface, and $\tau(\delta)$ the shear stress at the water/air interface.

For a stagnation point,

$$U_o = 2U_\infty \sin(s/R) \tag{9}$$

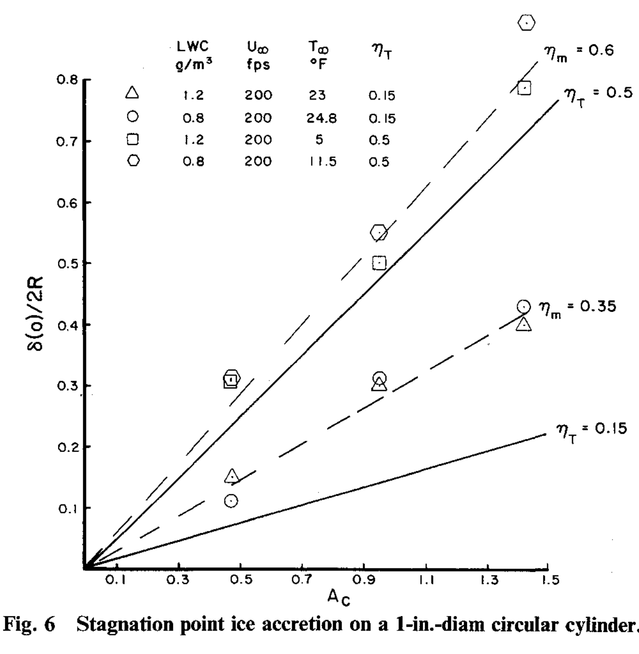

Fig. 6 Stagnation point ice accretion on a 1-in.-diam circular cylinder.

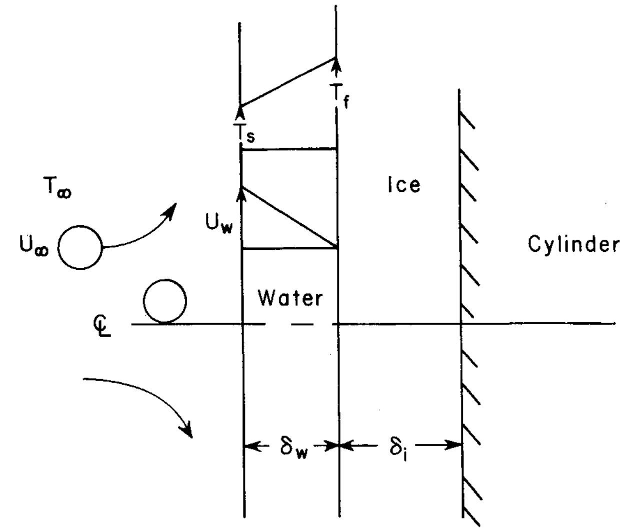

Fig. 7 Schematic of a stagnation/film-ice accretion model.

is the air potential flow along the surface of a cylinder. Assuming laminar flow (for demonstration purposes only), the stagnation point shear stress is given by Ref. 19:

$$\tau(s) = \frac{10.8}{\pi}\rho_a U_\infty^2 \sqrt{\frac{v_a}{RU_\infty}}\left(\frac{s}{R}\right) \tag{10}$$

$$\alpha = \pi/2 \tag{11}$$

where α is the angle between the drop trajectory and a tangent to the surface at impact.

To estimate the film thickness possible at a stagnation point, the given equations are solved for their zeroth-order expansion in distance from the stagnation point. It may be shown that the lowest-order effect is of the form

$$\frac{\delta_w(o)}{R} = \left(\frac{2}{\tau Re_w}\frac{LWC}{\rho_w}\right)^{1/2} \tag{12}$$

where

$$\tau = \frac{10.8}{\pi}\frac{\rho_a}{\rho_w}\frac{1}{Re^{1/2}}$$

$$Re = RU_\infty/v_a$$

$$Re_w = RU_\infty/v_w$$

At 200 ft/s, the film thickness on a cylinder with $2R = 1$ in. is estimated to be $\delta_w(o) \simeq 0.001$ in. or about 25 μm, which is nearly the diameter of the drop impacting the surface.

The preceding analysis, while admittedly approximate, does confirm that a thin film is anticipated over the ice when conditions of low freezing fractions are expected. These films may modify the freezing fraction as described by Messinger in a very direct way by providing surface roughness, which will augment the heat transfer as well as provide thermal resistance through which the latent heat of fusion must pass. Also, splashback from this layer cannot be ruled out. It should be noted that the Weber number, based on air dynamic pressure for a layer of this thickness, is of the order of 10^2, which suggests that the stripping of this film by the airstream may also occur.

It is significant to note at this time that Olsen et al.[20] photographed the microphysics of accretion at a stagnation point and had confirmed the presence of liquid and runback at the stagnation region. This work, however, indicates that liquid beading is also observed, suggesting that the surface tension neglected in the discussed analysis plays an important role. While from the photographs it is difficult to estimate the

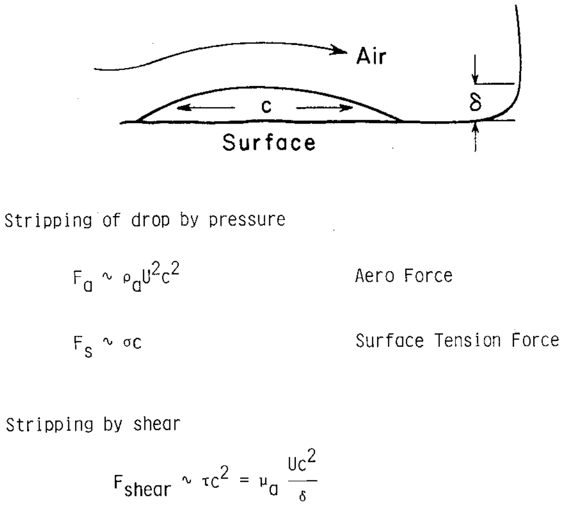

Fig. 8 Forces acting on a droplet attached to a surface.

height of the droplets, it is clear that when surface tension is acting, the film thickness estimates are low, and perhaps an effective droplet height at least an order of magnitude larger can be argued. This liquid roughness and, upon freezing, ice roughness is known to greatly affect the local convection heat transfer rate.[21] Detailed observations of the stagnation region have been made by Hansman and Turnock.[22]

VI. Freezing Fraction with Film Dynamics

Referring to Fig. 7, it is possible to develop a simple model to estimate the effect of the liquid film on the freezing fraction. Conserving mass and energy,

$$\frac{\mathrm{d}M_i}{\mathrm{d}t} = LWCU_\infty d^2 - \rho_w \frac{U_w}{2}\delta_w d \tag{13}$$

$$M_w = \delta_w d^2 \rho_w \tag{14}$$

$$E = h_{fs}M_i + \frac{M_w}{2}(T_s - T_f)C_{pw} \tag{15}$$

$$\frac{\mathrm{d}E}{\mathrm{d}t} = LWCd^2U_\infty\left(C_{pw}(T_\infty - T_f) + \frac{U_\infty^2}{2}\right) - \delta_w\frac{U_w\rho_w}{2}dC_{pw}\frac{(T_s - T_f)}{2} - q_\infty \tag{16}$$

A linear velocity and temperature profile has been assumed in the liquid film. The heat transfer from the air to the liquid film is

$$q_\infty = -h_c d^2\left(T_\infty + \frac{U_\infty^2}{2C_{pa}} - T_s\right) = -k_w d^2(T_s - T_f)/\delta_w \tag{17}$$

The system of equations is closed when the shear stress on the film by the airstream is equated to the shear stress in the film

$$\tau_\infty = \mu_w U_w/\delta_w \tag{18}$$

It is curious that in the vicinity of the stagnation point it may be shown that the shear stress dominates the pressure gradient for thick layers. It is straightforward to solve for Eqs. (13–18) for

$$\eta = \frac{\mathrm{d}M_i}{\mathrm{d}t}\Big/ LWCU_\infty d^2 = \frac{C_{pw}(T_\infty - T_f)}{h_{fs}} - \frac{q_\infty}{h_{fs}LWCU_\infty d^2} + \frac{C_{pw}(1-\eta)\delta_w q_\infty}{2h_{fs}k_w d^2} \tag{19}$$

The first two terms are the freezing fraction as described by Messinger. The last term, which is proportional to the film thickness, reduces the freezing fraction as a consequence of the presence of the film. Dividing the Messinger heat-transfer term into this film term yields the importance of the film in the thermodynamics. This ratio is

$$(\delta_w LWCU_\infty C_{pw})/k_w$$

Therefore, at a liquid water content of 1 gm/m^3 and at cruise, this ratio is about

$$0.02\,\delta_w(\mathrm{mil})$$

With a 1-mil and 10-mil film layer, the effective heat transferred to the freestream is reduced by 2 or 20%, respectively. This order-of-magnitude analysis indicates that a uniform film analysis correction to the freezing fraction concept is not sufficient to account for the observed differences between measured and predicted stagnation point ice accretion. Augmentation of the convective heat transfer coefficient by liquid beading and ice roughness and errors in estimating the accumulation parameter, possibly by splashback, are primary candidates.

VII. Film Beading

It has been suggested that liquid film breakdown and film beading are mechanisms that are suspected to influence the freezing fraction. The growth of a droplet attached to a surface in a stream will be controlled by π parameters 12, 17, and 18. Figure 8 schematically shows a droplet on a surface exposed to an airstream. The force holding the droplet to the surface is surface tension and is of the order

$$F_s \sim \sigma C \tag{20}$$

Both shear τ and aerodynamic forces strip the droplet from the surface:

$$F_{\text{shear}} \sim \tau C^2$$

$$F_a = \rho_a U_\infty^2 C^2$$

By obtaining the ratio of the surface tension force to the aero- and shear stress forces on the droplet, it is easy to show that to properly scale droplet stripping, it is necessary to hold

$$\pi_{17} = (U_\infty C/\nu_a) \quad \text{(Reynolds number)}$$

$$\pi_{18} = (\rho_a U_\infty^2 C/\sigma_{w/a}) \quad \text{(Weber number)}$$

$$\pi_{12} = \gamma \quad \text{(Contact angle)}$$

constant between scaled tests. If subscripts 1 and 2 denote tests at two geometric scales,

$$\frac{U_1}{U_2} = \frac{C_2}{C_1}, \quad \frac{\sigma_{w/a\,2}}{\sigma_{w/a\,1}} = \frac{C_1}{C_2}, \quad \text{and} \quad \gamma_1 = \gamma_2$$

These icing tests can be undertaken using the A_C and η scaling laws. The surface tension can be changed using a surface active agent that does not change the freezing temperature, and the contact angle can be held constant by changing the airfoil material. It is finally noted that Hansman and Turnock[22] have completed tests that repeated two icing conditions in a wind tunnel where the only difference in tests added a surfactant to the upstream spray. Very significant differences in the accreted ice pattern were noted, strongly supporting our conjecture that icing tests must scale properly the microphysics of liquid film dynamics and bead formation.

VIII. Conclusions

It is argued that improved ice accretion scaling may require a better match in Reynolds number and more accurate consideration of the physics of water film and droplet dynamics on the airfoil surface. Additional scaling parameters are proposed which require that the surface tension phenomenon be more accurately accounted for in wind-tunnel tests. An unfortunate fact is that if proposed additional scaling parameters prove to meet the requirements for conducting improved subscale icing tests, wind-tunnel subscale tests are likely to be even more restrictive.

Lastly, the phenomenon of droplet splashback cannot be ruled out, and there is little justification for going to great care in computing the impacting of droplets with a surface if significant splashback occurs. It is strongly recommended that tests be conducted in the near future to examine the question of splashback.

Acknowledgments

This work was supported in part by the FAA and NASA Lewis through Contract NAS1-18302. The author gratefully acknowledges internal support from Continuum Dynamics, Inc., which permitted completion of this effort. The author would like to thank R. John Hansman Jr. of the Massachusetts Institute of Technology for providing an advanced copy of his manuscript.

References

[1]Dunham, R. E., Bezos, G. M., Gentry, C. L., and Melson, E., "Two-dimensional Wind Tunnel Tests of a Transport-Type Airfoil in a Water Spray," AIAA Paper 85-0258, Jan. 1985.

[2]Feo, A., "Rotating Arms Applied to Studies of Single Angular Drop Impacts," AIAA Paper 87-0257, Jan. 1987.

[3]Bragg, M. B., Gregorek, G. M., and Shaw, R. J., "An Analytical Approach to Airfoil Icing," AIAA Paper 81-0403, Jan. 1981.

[4]Papadakis, M., Elangovan, R., Freund, G. A., Jr., and Breer, M.D., "Experimental Water Droplet Impingement Data on Two-Dimensional Airfoils, Axisymmetric Inlet and Boeing 737-300 Engine Inlet," AIAA Paper 87-0097, Jan. 1987.

[5]Guibert, A. G., Janssen, E., and Robbins, W. M., "Determination of Rate, Area, and Distribution of Impingement of Waterdrops on Various Airfoils from Trajectories Obtained on the Differential Analyzer," NACA Rept. RM 9A05, Feb. 1949.

[6]Ruff, G. A., "Development of an Analytical Ice Accretion Prediction Method (LEWICE)," Sverdrup Technology, Inc., LeRC Group Progress Report, Feb. 1986.

[7]MacArthur, C. D., "Numerical Simulation of Airfoil Ice Accretion," AIAA Paper 83-0112, Jan. 1983.

[8]Lozowski, E. P., Stallabrass, J. R., and Hearty, P. F., "The Icing of an Unheated, Nonrotating Cylinder. Part I: A Simulation Model," *Journal of Climate and Applied Meteorology*, Vol. 22, Dec. 1983, pp. 2053–2062.

[9]Bilanin, A. J., "Scaling Laws for Testing Airfoils Under Heavy Rainfall," *Journal of Aircraft*, Vol. 24, Jan. 1987, pp. 31–37.

[10]"Aircraft Ice Protection," Department of Transportation Federal Aviation Administration Advisory Circular 20–73, April 1971, pp. 29–42.

[11]Messinger, B. L., "Equilibrium Temperature of an Unheated Icing Surface as a Function of Airspeed," *Journal of Aeronautical Sciences*, Jan. 1953.

[12]Ruff, G. A., "Analysis and Verification of the Icing Scaling Equations, Analysis and Verification," AEDC Rept. TR-85-30, Vol. II, March 1986.

[13]Hauger, H. H., and Englar, K. G., "Analysis of Model Testing in an Icing Wind Tunnel," Rept. SM14933, Douglas Aircraft Co., Inc., 1954.

[14]Sibley, P. J., and Smith, R. E., Jr., "Model Testing in an Icing Wind Tunnel," Rept. LR10981, Lockheed Aircraft Corp., 1955.

[15]Dodson, E. O., "Scale Model Analogy for Icing Tunnel Testing," Document D66-7976, Boeing Airplane Co., Transport Division, March 1962.

[16]Jackson, E. T., "Development Study: The Use of Scale Models in an Icing Tunnel to Determine the Ice Catch on a Prototype Aircraft with Particular Reference to Concorde," SST/B75T/RMMcK/242, British Aircraft Corp. (Operating) Ltd., Filton Division, July 1967.

[17]Armand, C., Charpin, F., Fasso, G., and Leclere, G., "Techniques and Facilities Used at the Onera Modane Centre for Icing Tests," AGARDograph AF-127, Nov. 1978.

[18]Ruff, G. A., "Analysis and Verification of the Icing Scaling Equations, Analysis and Verification, AEDC Rept. TR-85-30, Vol. I, March 1986.

[19]Schlicting, D., *Boundary-Layer Theory*, McGraw-Hill Book Co., New York, 1968.

[20]Olsen, W., Shaw, R. J., and Newton, J., "Ice Shapes and the Resulting Drag Increase for a NACA 0012 Airfoil," NASA TM 83556, Jan. 1984.

[21]Achenbach, E., "The Effect of Surface Roughness on the Heat Transfer from a Circular Cylinder to the Cross Flow of Air," *International Journal of Heat Mass Transfer*, Vol. 20, April 1977, pp. 359–369.

[22]Hansman, J. R., Jr. and Turnock, S. R., "Investigation of Surface Water Behavior During Glaze Ice Accretion," AIAA Paper 88-0015, Jan. 1988.

Notice to Subscribers

We apologize that this issue was mailed to you late. The AIAA Editorial Department has recently experienced a series of unavoidable disruptions in staff operations. We will be able to make up some of the lost time each month and should be back to our normal schedule, with larger issues, in just a few months. In the meanwhile, we appreciate your patience.